Quaternary Research 77 (2012) 149–158

Contents lists available at SciVerse ScienceDirect

Quaternary Research

journal homepage: www.elsevier.com/locate/yqres

Development of unusual rock weathering features in the Cordillera Blanca, Peru

Donald T. Rodbell [a,*], Holli M. Frey [a], Matthew R.F. Manon [a], Jacqueline A. Smith [b], Nicholas A. McTurk [a]

[a] Geology Department, Union College, Schenectady, NY 12308, USA
[b] Department of Physical & Biological Sciences, The College of Saint Rose, Albany, NY 12203, USA

ARTICLE INFO

Article history:
Received 30 December 2010
Available online 19 October 2011

Keywords:
Rock weathering
Moraine dating
Exposure ages
Tropical glaciation

ABSTRACT

Mylonite textures in granodiorite boulders are responsible for higher rates of surface denudation of host rocks and the progressive development of unusual rock weathering features, termed *weathering posts*. These textures are characterized by smaller grain sizes, higher biotite content, and a higher biotite axial ratio in host rocks relative to weathering posts. Elemental concentrations do not show a significant difference between weathering posts and the host rocks in which they are found, and this reflects the absence of a weathering residue on the rock surfaces. Chemical weathering loosens the bonds between mineral grains through the expansion of biotite, and the loosened grains fall off or are blown off the boulder surface and continue their chemical alteration in the surrounding soil. The height of weathering posts on late Quaternary moraines increases at a linear rate of ~1.45 ± 0.45 cm $(1000\ \mathrm{yr})^{-1}$ until post heights reach the diameter of host rocks. Such a rate of boulder denudation, if unrecognized, would generate significant errors (>20%) in cosmogenic exposure ages for Pleistocene moraines. Given the paucity of boulders with diameters that significantly exceed 1.5 m, the maximum age of utility of weathering posts as a numeric age indicator is ~100 ka.

Introduction

Rock-weathering features such as rinds, pits, and clast grussification have long been used as a basis for correlating and subdividing deposits in glaciated terrain (e.g., Blackwelder, 1931; Birkeland, 1973, 1974; Burke and Birkeland, 1979; Burbank and Cheng, 1991). Even when rates of rock weathering are not known, the relative degree of rock weathering can provide an important and objective means of subdividing deposits according to *relative* age (Birkeland et al., 1979). In several notable cases (e.g., Pierce et al., 1976; Colman and Pierce, 1980; Colman, 1981; Chinn, 1981; Whitehouse et al., 1986), workers have measured the extent of rock-weathering development on independently dated landforms, and have successfully determined rates of development of rock-weathering features. In these cases, the rock-weathering features themselves can then be used as a numeric ('absolute') dating tool for a given region. The widespread use of cosmogenic radionuclides (CRN; Gosse and Phillips, 2001) to date late Quaternary landforms has lessened the importance of rock-weathering features as dating tools. However, inasmuch as the application of CRN dating depends, in part, on an understanding of rock-weathering rates, and independently measured weathering rates are often unavailable, erosion rates must be assumed for purposes of age calculation (Gosse and Phillips, 2001). Rarely have such assumptions been tested rigorously.

One of the few applications of rock-weathering features to subdivide glacial deposits in the Andes Mountains comes from the Cordillera Blanca, Peru (Fig. 1). Here, Clapperton (1981) used the presence of weathering "residuals" on granodiorite boulders to assign a "pre-Wisconsin" age to moraines on the western side of the range. Subsequently, Rodbell (1993) measured these weathering residuals (hereafter termed *weathering posts*) on a variety of late Quaternary moraines, and documented the progressive development of these odd features (Fig. 2). The advantage of weathering posts as a dating tool is that they are ubiquitous on moraines in drainage basins where the Cordillera Blanca batholith has been exposed by glacial erosion, they are visible from distances of many tens of meters, and their heights can be measured rapidly. Rodbell (1993) advocated using the mean of the five tallest posts on individual moraine ridges as an index of moraine age. This metric was intended to avoid the effects of variations in rock type, microclimate, fire history, and boulder exhumation that may influence the average degree of rock weathering on any given moraine. Rodbell (1993) reported that weathering posts are present only on pre-Holocene moraines; post heights are 12 ± 2 cm ($\pm 1\sigma$; n = 542) on late glacial (*Manachaque*) moraines, 23 ± 2 cm (n = 899) on moraines of the local last glacial maximum (*Laguna Baja*), and 42 ± 5 cm (n = 899) and 66 ± 5 cm (n = 119) on undated older *Rurec* and *Cojup* moraines. Though post heights clearly increase with moraine age, Rodbell's (1993) attempt to calibrate weathering-post development with time was limited by a lack of absolute age control for the older three moraine groups (*Laguna Baja*, *Rurec*, and *Cojup*). Furthermore, no petrologic or geochemical

* Corresponding author. Fax: +1 518 388 6417.
E-mail address: rodbelld@union.edu (D.T. Rodbell).

0033-5894/$ – see front matter © 2011 University of Washington. Published by Elsevier Inc. All rights reserved.
doi:10.1016/j.yqres.2011.09.004

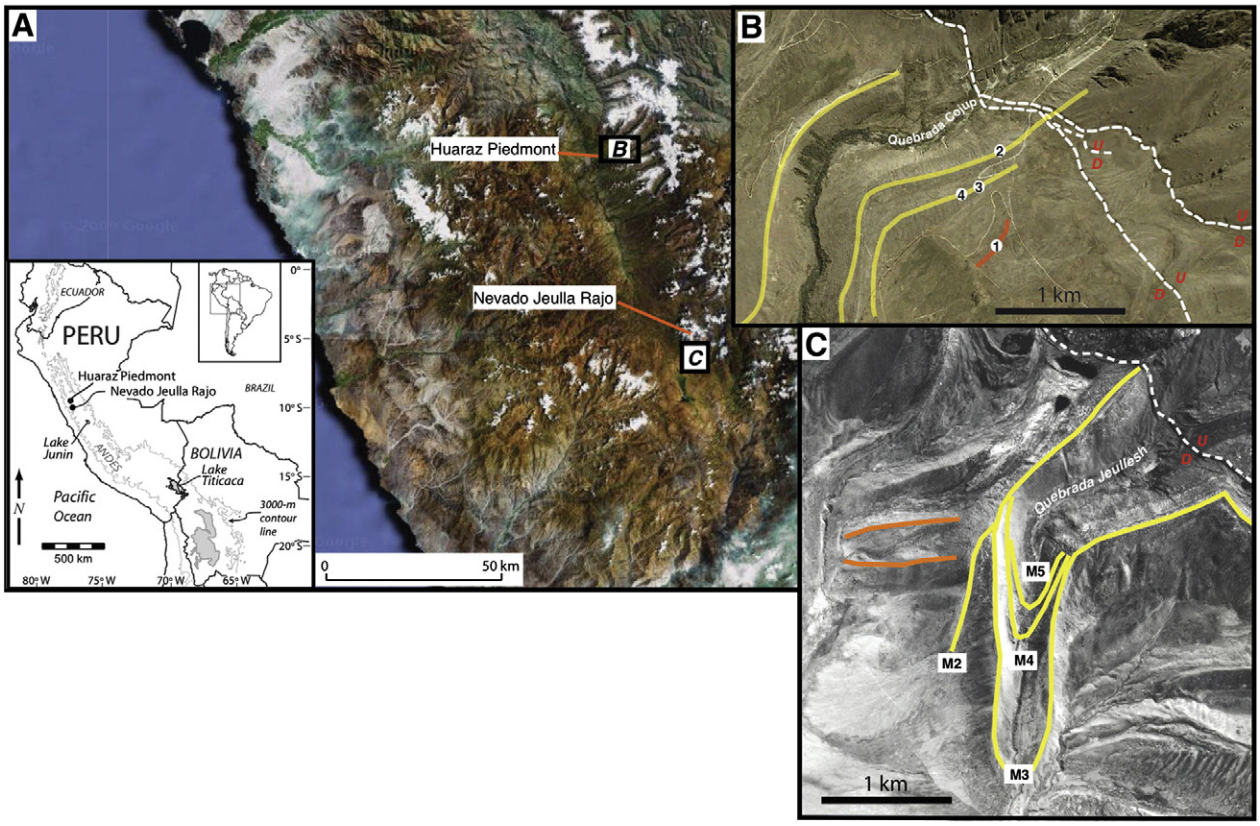

Figure 1. Location of the study sites on the west side of the Cordillera Blanca in central Peru (*A*); satellite image is from Google Earth 29 July, 2010. (*B*) Simplified moraine map of the piedmont above the village of Huaraz, Peru (from Rodbell, 1993); yellow and orange lines are Rurec and Cojup moraine crests, respectively; white dashed line in *B* and *C* is Cordillera Blanca Normal Fault (Schwartz, 1988); *U* and *D* refer to upthrown and downthrown sides, respectively, of the west-dipping normal fault. (*C*) Simplified moraine map of Quebrada Jeullesh on the west side of the Nevado Jeulla Rajo massif in the southernmost Cordillera Blanca (from Smith and Rodbell, 2010). Base map for *B* is Google Earth 29 July, 2010 and that for *C* is aerial photograph 3341 (Instituto Geográfico Militár, Lima Peru).

explanation for the differential weathering required for development of weathering posts in apparently lithologically homogeneous boulders has been provided.

In this paper, we report results of a petrologic and geochemical study of weathering posts and host rocks in an attempt to understand the origin of the differential rock weathering that leads to post development in what appear to be homogeneous granite/granodiorite boulders. Farber et al. (2005) and Smith and Rodbell (2010) report over 100 exposure ages for boulders on moraine crests on the west side of the Cordillera Blanca. Using this CRN-based dataset and the radiocarbon chronology of Rodbell (1992, 1993), we also report a calibration dataset for weathering-post development.

Study area

The Cordillera Blanca forms a ~225-km-long portion of the northwest–southeast trending continental divide in northern Peru (Fig. 1). With numerous peaks standing in excess of 6000 m, including the highest peak, Nevado Huascarán Súr (6768 m), the Cordillera Blanca is the most extensively glaciated tropical mountain range in the world today. The core of the range is primarily Tertiary granodiorite, whereas the east and west flanks are upper Mesozoic metasedimentary rocks that include, amphibolite, hornfels, quartzite, and limestone (Wilson et al., 1967; Servicio Nacional de Geología y Minería, 1970). Felsic volcanic rocks are locally abundant in the southern part of the range. Glaciation has stripped the metasedimentary cover from the headwaters of many drainages, thus exposing the underlying granite and/or granodiorite. Moraines in these catchments are composed of a mixture of clast lithologies, and in any one catchment younger moraines are composed of a greater percentage of granite and/or granodiorite clasts than are older moraines (Rodbell, 1991). Whereas many of the granite/granodiorite boulders possess weathering posts, the quartzite and felsic volcanic boulders are commonly devoid of weathering features, and most quartzite boulders still possess glacial polish and striae. The west-dipping Cordillera Blanca Normal Fault runs along the western side of the massif, offsetting many pre-Holocene moraine crests (Schwartz, 1988).

Approximate mean annual temperature and precipitation for sites above 3000 m on the west side of the range are 6.7°C and 71 cm, respectively (Rodbell, 1992). There is little seasonal variation in temperature but precipitation is strongly seasonal; the dry season extends from May through October, and on average only ~20% of the total annual precipitation falls during these 6 months. Diurnal temperature variations are large; at 4000 m, diurnal temperature ranges are 10–13.5°C and these increase with elevation (Smith, 1988). Vegetation on Pleistocene moraines is primarily tussock grasses, sclerophyllous shrubs, and giant rosettes (Smith, 1988).

Methods

Field

To augment the data set of ~2500 post heights reported by Rodbell (1993), we measured the height (to the nearest 1 cm) of ~350 weathering posts on boulders on moraine crests on the southwestern side of the Nevado Jeulla Rajo Massif in the southern Cordillera Blanca (Figs. 1*A* and *C*). These are some of the same moraines that were

https://doi.org/10.1016/j.yqres.2011.09.004 Published online by Cambridge University Press

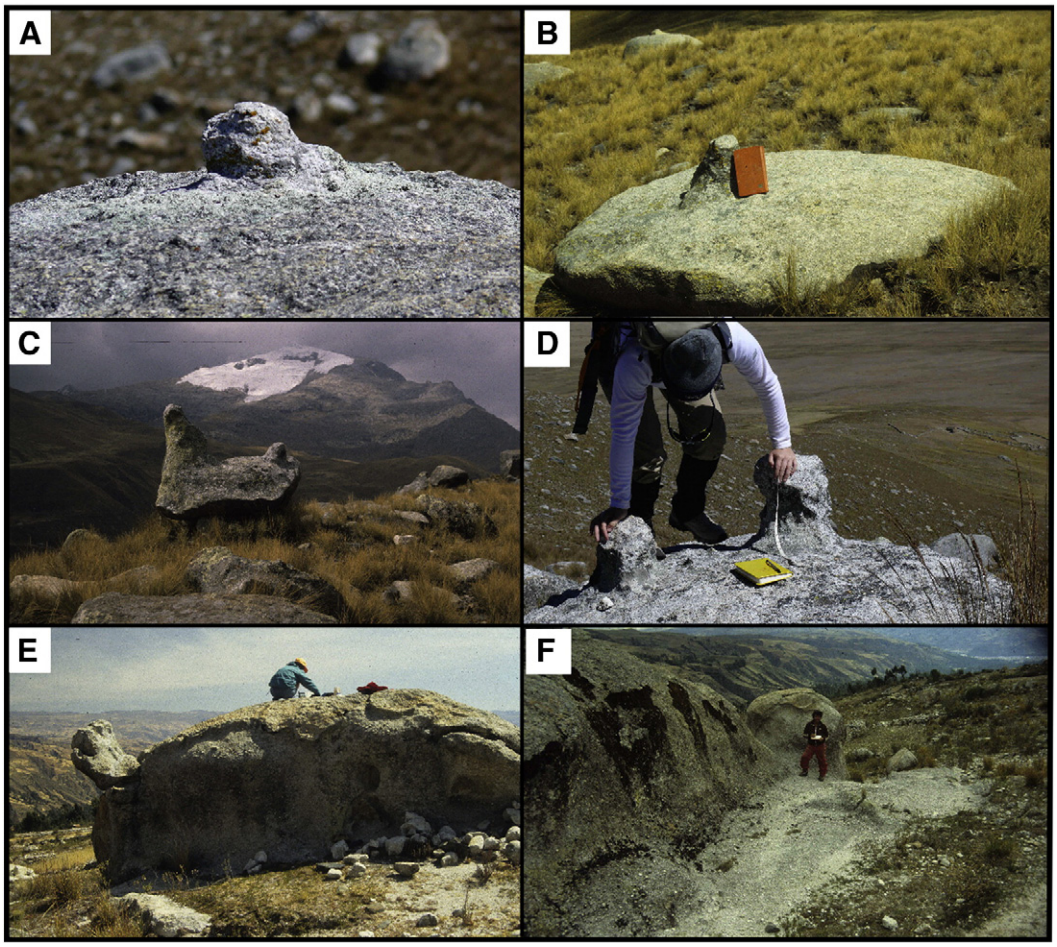

Figure 2. The progressive development of weathering posts on moraines of increasing age (A.–F.). A Incipient weathering post (~10 cm tall) on a late glacial (~10 ka) moraine; B. A 25-cm tall post on a ~30 ka moraine; C. A 45-cm tall post on a ~30 ka moraine; D. A ~40-cm tall post on a ~30 ka moraine; E. A ~65-cm tall post on an a ~75 ka moraine, and F. A 1.5-m tall post (behind individual) on a >400 ka moraine.

dated using CRN analysis by Smith and Rodbell (2010). Three intact weathering posts were sampled with a sledge hammer in the Jeulla Rajo Massif region, and a total of 17 drill core samples (~4–5 cm long and 2 cm in diameter) comprising four sample suites were obtained from four boulders (Fig. 1*B*) containing prominent weathering posts in the glaciated piedmont above the village of Huaraz (Fig. 1*A*). The drill-core samples were taken from the same moraines included in the weathering-post study of Rodbell (1993) and in the exposure-dating study of Farber et al. (2005). Seven of the core samples came from the top of weathering posts and 13 came from host rocks at various distances from posts (Table 1).

Laboratory

Petrographic analysis was done on eighteen standard thin sections (9 weathering post samples and 9 host rocks) to assess modal abundances, grain size, and textures. Proportions of mineral phases were determined by point counting (≥1200 points per slide). Using a Zeiss EVO50XVP scanning electron microscope, a mosaic of backscattered electron (BSE) images was made from each thin-section to elucidate textural and grain size differences between the weathering post and their host rocks. Length and width of all plagioclase and biotite grains were measured using ImageJ software. A minimum of 100 plagioclase and 38 biotite crystals were measured in each sample. The plagioclase grain-size variations are presented with respect to grain area, whereas the grain shape of biotite is reported as axial ratios.

All samples were analyzed for whole-rock major elements by ICP-MS (OES) at Acme Laboratories, Vancouver Canada. Trace elements were analyzed by ICP-MS at Union College, using four calibration standards (BIR-1, NIST-688, BCR-2, and NIST-278), following complete sample dissolution by hydrofluoric and nitric acids.

Results

Petrology

The samples straddle the granite/granodiorite fields, with abundant plagioclase (28–50%) and quartz (31–52%), and subordinate orthoclase (7–32%) (Table 2; Fig. 3). There do not appear to be any systematic trends of modal abundances with sample type (post or host rock). The heterogeneity in the samples is clearly demonstrated by replicate thin-sections of a single post from sample suite 1 (Table 1; Fig. 3, solid circles), which span a significant compositional range. In addition to the major mineral phases, all samples contain biotite and muscovite. Additional accessory phases in some samples include titanomagnetite ± ilmenite ± zircon ± apatite ± sphene ± secondary chlorite ± secondary epidote. Myrmekitic intergrowths of quartz and albite were also present.

Despite the assemblage and modal similarities, there are significant textural differences between the post and host rock samples, as shown in pairs of photomicrographs from three sample suites (Fig. 4). Typically, the post samples feature a coarse crystalline texture, with large interlocking crystals of equant plagioclase, quartz, and orthoclase, and lesser biotite (2.6–3.6%). The plagioclase commonly displays oscillatory zoning and occasional complex overgrowths on corroded cores. The quartz appears pristine, with minimal strain shadows. The orthoclase has abundant perthitic exsolution and is more fretted on its

https://doi.org/10.1016/j.yqres.2011.09.004 Published online by Cambridge University Press

Table 1
Weathering post and host rock samples obtained for this study.

Valley	Sampling site	Sample suite	Sample number	Date collected	Type of sample	Location on rock	Notes
Quebrada Cojup	Left-lateral Cojup moraine	1	R93PE1	8/8/93	Drill core	Top of 66-cm tall weathering post	Approximate GPS location: 9°29.76′S; 77°27.43′W; 3775 masl
			R93PE2	8/8/93	Drill core	Top of 66-cm tall weathering post	
			R93PE3	8/8/93	Drill core	Top of 66-cm tall weathering post	
			R93PE4	8/8/93	Drill core	10 cm from base of post	
			R93PE5	8/8/93	Hand sample	100 cm from base of post	
			R93PE6	8/8/93	Hand sample	100 cm from base of post	
			R93PE8	8/8/93	Drill core	100 cm from base of post	
Quebrada Cojup	Left-lateral Rurec moraine	2	R93PE12	8/10/93	Drill core	Top of 20-cm tall weathering post	Approximate GPS location: 9°29.42′S; 77°27.49′W; 3850 masl
			R93PE10	8/10/93	Drill core	20 cm from base of weathering post	
			R93PE11	8/10/93	Drill core	21 cm from base of weathering post	
Quebrada Cojup	Left-lateral Rurec moraine	3	R93PE14	8/10/93	Drill core	Top of 25-cm tall weathering post	Approximate GPS location: 9°29.42′S; 77°27.47′W; 3830 masl
			R93PE15	8/10/93	Drill core	25 cm from base of post	
			R93PE16	8/10/93	Drill core	60 cm from base of post	
Quebrada Cojup	Left-lateral Rurec moraine	4	R93PE17	8/10/93	Drill core	top of 25-cm tall weathering post	Approximate GPS location: 9°29.42′S; 77°27.47′W; 3830 masl
			R93PE18	8/10/93	Drill core	Top of 25-cm tall weathering post	
			R93PE19	8/10/93	Drill core	25 cm from base of post	
			R93PE20	8/10/93	Drill core	50 cm from base of post	
Quebrada Jeullesh	Right-lateral M3 moraine		PE09-POST 1	6/30/09	Full post	Full post, 25-cm tall	Boulder is 80-cm long; 50 cm wide; 40 cm tall; 10°00.017′S; 77°16.301′W; 4452 masl
	Right-lateral M2 moraine		PE09-POST 2	6/30/09	Full post	Full post, 26-cm tall	Boulder is 275-cm long; 106 cm tall; 10°00.153′S; 77°16.397′W; 4392 masl
	Left-lateral M4 moraine		PE09-POST 3	6/30/09	Full post	Full post, 17-cm tall	Boulder is 140-cm long; 40 cm tall; 10°00.401′S; 77°16.′W; 4289 masl

edges than the other major phases. The biotite is mostly tabular and similar in size to the felsic phases.

The host rock samples have a much more heterogeneous texture that is typified by smaller plagioclase, elongate biotite/muscovite and ribbon quartz. In general, these samples have a deformed fabric, with abundant fractured plagioclase and orthoclase phenocrysts, strained or recrystallized quartz crystals, and secondary muscovite and chlorite along grain boundaries, in fractures, and as alterations on margins of biotite. The plagioclase in all samples spans a range of sizes (up to 10 mm^2), but averages 20–50% smaller in the host rock samples (Table 2). The histograms of plagioclase area show that the post samples have a smaller peak and broader distribution than the host-rock samples, due to the presence of more large crystals (Fig. 5). The host-rock samples have a greater proportion of small grains, with ~60%<0.8 mm^2. The quartz crystals are also smaller in the host-rock samples, featuring a mosaic texture of polycrystalline aggregates, with lensoid forms. In contrast, orthoclase is not smaller in the host-rock samples, with some porphyroblasts up to 5 cm in length. Biotite is slightly more abundant in the host-rock samples (2.4–5.9%) than in the post samples (2.6–3.6%). In the host-rock samples, biotite is curvilinear or elongate, often mantling large orthoclase phenocrysts or intergrown with veins of microcrystalline quartz. This difference in biotite morphology was quantified using axial ratios, which average 2.6 for the post samples and 3.1 for the host-rock

Table 2
Modal abundances of weathering posts and host rocks.

Sample suite (Table 1)	Sample	Distance from post (cm)	Quartz	Plagioclase	Orthoclase	Biotite	Muscovite	Fe–Ti Ox
			Percentage of total					
1	R93PE1	0	31.1	37.3	28.7	2.7	0.1	0.1
	R93PE2	0	36.2	41.9	18.1	2.9	0.3	0.0
	R93PE3	0	30.1	46.1	19.7	3.6	0.4	0.0
	R93PE4	10	29.5	34.8	30.2	4.9	0.2	0.0
	R93PE8	125	29.4	47.9	18.0	4.5	0.0	0.0
2	R93PE12	0	42.8	32.0	21.2	3.3	0.7	0.0
	R93PE10	20	42.2	36.3	18.4	2.4	0.6	0.1
	R93PE11	20	32.0	45.6	17.2	3.8	1.2	0.2
3	R93PE14	0	46.3	44.1	6.4	2.7	0.0	0.0
	R93PE15	25	49.1	32.4	12.7	5.5	0.2	0.1
	R93PE16	60	46.9	26.9	22.1	3.5	0.2	0.0
4	R93PE17	0	31.8	43.4	20.5	2.9	1.1	0.0
	R93PE18	5	43.7	38.6	12.3	4.4	0.7	0.3
	R93PE19	25	43.4	29.1	19.2	5.9	1.5	0.8
	R93PE20	50	35.2	30.6	29.5	3.3	0.8	0.3

Modal abundances based on >1200 points per slide.
Other phases present in trace amounts: sphene, apatite, zircon, chlorite, epidote.

https://doi.org/10.1016/j.yqres.2011.09.004 Published online by Cambridge University Press

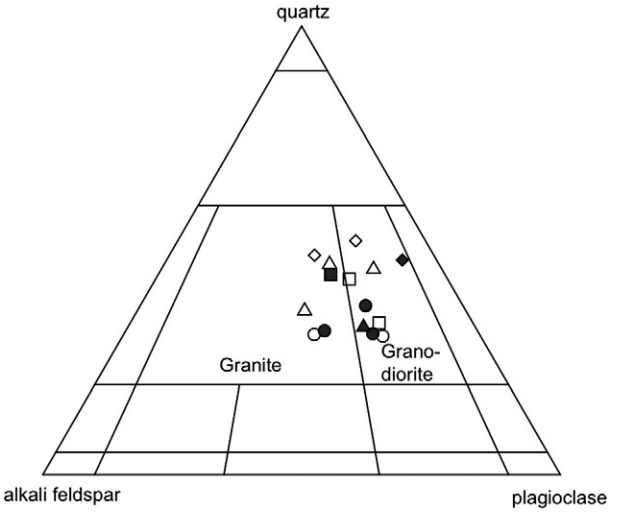

Figure 3. Modal classification of post (closed symbols) and host-rock samples (open symbols) shows all samples plot in the granite and granodiorite fields. Suite 1 (Table 1) is denoted by circles, suite 2 by diamonds, suite 3 by squares, and suite 4 by triangles.

samples (Fig. 6; Table 3). In the host-rock samples, there is typically a higher proportion of elongate biotite grains, and this is seen most strongly in samples from suite 1 (Fig. 6; Table 3).

Geochemistry

Major element and trace element concentrations do not show any consistent trends between weathering posts and host-rock samples (Table 3; Fig. 6).

Discussion

Textural heterogeneity and the development of mylonites

Solid-state deformation fabrics overprint magmatic fabrics throughout the host samples, suggesting ductile deformation after emplacement. Given the grain-size reduction and strongly foliated fabric in the host rock samples, they can be categorized as mylonites (e.g., Vernon et al., 1983; Gapais, 1989). In granites, fluids and the contrasting structures of the minerals can lead to localized deformation. In otherwise relatively homogeneous bodies, mylonites may develop with the introduction of water along cracks or grain-boundary weaknesses (Segall and Simpson, 1986). Quartz, due to its non-isotropic structure, flows easily and recrystallizes into fine-grained aggregates or ribbons, whereas feldspars undergo minimal plastic deformation before brittle fracture. Commonly, feldspar porphyroblasts show minor recrystallization along their margins and are surrounded by anastomosing quartz and mica. Cracks or pore spaces develop, which localize fluids and can lead to enhanced chemical weathering. Evidence for this are myrmekitic intergrowths, which have been linked to the deformation of granites, and when found with muscovite, indicate the presence of fluids (Vernon et al., 1983).

Within the Cordillera Blanca Batholith, evidence of both macroscopic (i.e., layering, biotite schlierin) and microscopic (mylonites) ductile and brittle deformation have been documented, with intensity greatest along the western margin and boundary with the Cordillera Blanca Normal Fault (e.g., Atherton and Sanderson, 1987, Petford and Atherton, 1992), which is the region of this study. Based on field relations, geochemical, and isotopic evidence, Atherton and Sanderson (1987) suggested that the Cordillera Blanca Batholith is a nested batholith, comprising at least five units ranging from diorite to tonalite to granodiorite, in which the younger members intrude older units. The emplacement of these plutonic bodies has led to solid-state deformation fabrics which grade into brittle cataclasites towards the western fault-bounded margin of the batholith (Petford and Atherton, 1992). The ascent of the various magma bodies is thought to be fault-controlled via dyke-like conduits, with some high strain related to uplift along the fault.

Weathering-post formation

Differential weathering between posts and host boulders is responsible for the formation of these columnar features on late Quaternary moraines. The distinctive localized mylonite texture in the host-rock samples likely allowed for pore-water migration and accelerated chemical weathering. The greater elongation of the biotite grains in the host-rock samples would also promote increased rates of chemical weathering on the host boulders due to an increased surface area available for grain-boundary weathering. White (2002) cited the weathering, and subsequent volumetric expansion of biotite, as the principal force contributing to the physical decomposition of the Panola Granite in the southeastern United States. The alteration of biotite into secondary minerals of a larger volume, such as muscovite or chlorite, enhances fracturing along grain boundaries and pre-existing weaknesses, thus allowing for rapid granite disintegration (Eggler et al., 1969). These micro-fractures, which are apparent in the host rock samples, can be infiltrated by various weathering solutions, thereby increasing the overall weathering rate (Bland and Rolls, 1998).

The smaller average plagioclase grain size and microcrystalline quartz veins in the host rock samples also likely allow for the increased rates of weathering in the host boulders. Smaller average grain sizes would produce increased availability for grain boundary weathering, as the surface area to volume ratio of these small grains is greater than that for larger mineral grains. Typically, a rock structure containing small mineral grains that are poorly sorted, such as the host-rock samples, is able to resist the effect of water and other weathering solutions due to their decreased porosity compared to well-sorted, large-grain textures (Bland and Rolls, 1998). However, the alteration and elongation of biotite grains in these samples that result in micro-fractures in the rock texture would act to increase the permeability of the host boulder and allow for weathering solutions to rapidly degrade the smaller grains.

The weathering post samples contain an interlocking mosaic of large plagioclase, quartz and orthoclase grains that would result in decreased permeability, and there are few grain-boundary vacancies in this crystalline mosaic. The biotite grains also have a smaller axial ratio, corresponding to a more euhedral shape, compared to the ribbons of elongated biotite in host-rock samples. Therefore, even though the biotite in the post samples shows some alteration, it does not produce long fractures through which pore water can percolate.

One of the curiosities of weathering posts as defined here is the paucity of reports of such features from other regions. Differential rock weathering has been reported from many regions, but the formation of columnar posts up to ~1 m in height in granitic rocks is indeed a rarity. We have noted isolated occurrences of such features on diorite erratics in the central and southern Peruvian Andes but neither the abundance of such features nor their degree of development is comparable to weathering-post development on the west side of the Cordillera Blanca. Apparently, the combination of lithology, textural heterogeneity, and range of climatic conditions that have been present on the west side of the Cordillera Blanca has been ideal for the formation of weathering posts.

Chemical weathering

Although physical weathering and grussification of the granite boulders is well-developed, these processes are not accompanied by

https://doi.org/10.1016/j.yqres.2011.09.004 Published online by Cambridge University Press

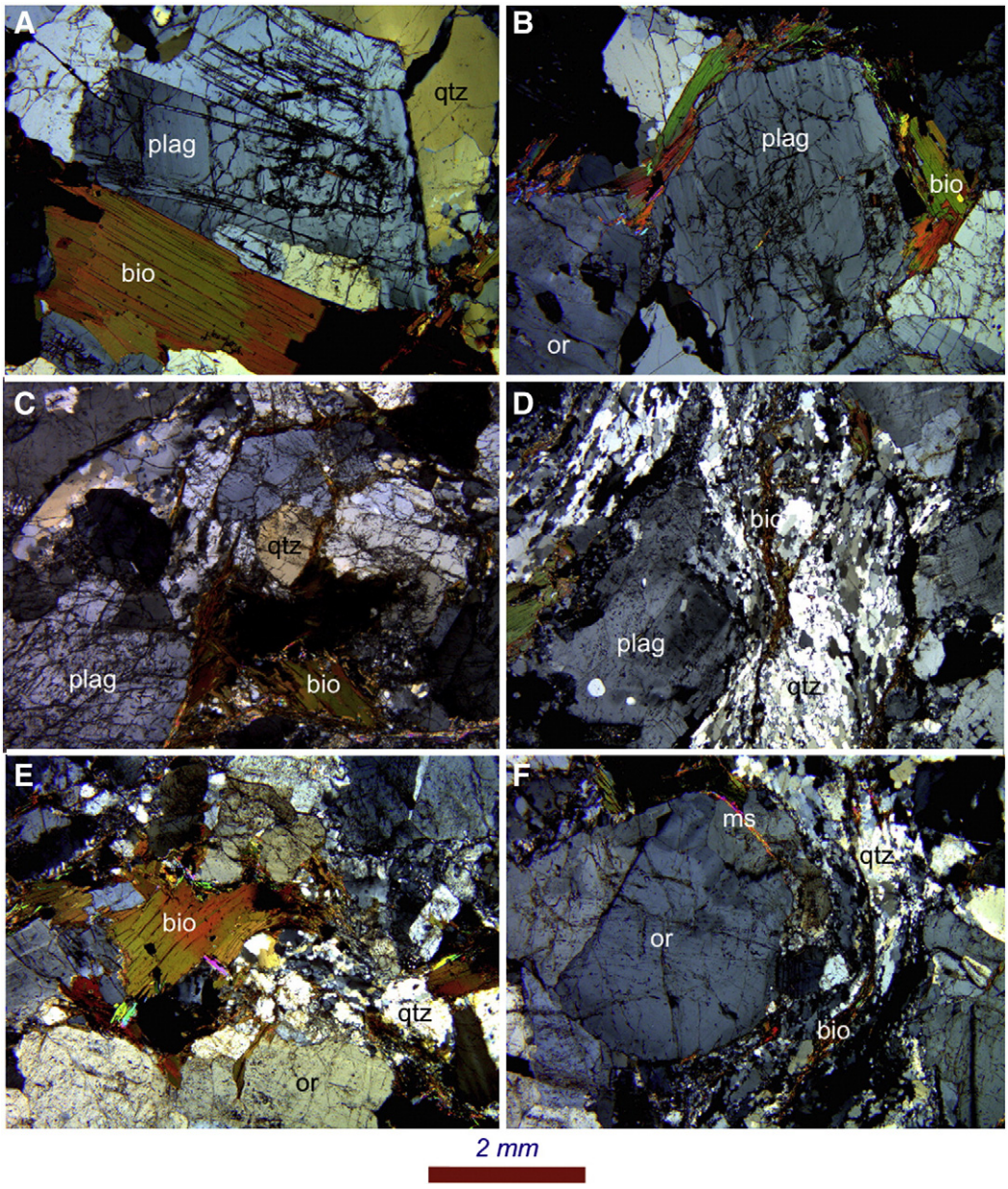

Figure 4. Photomicrographs of post samples (left column) and host rock samples (right column) highlight the textural differences in the samples. Sample pairs are from the same glacial erratic; A/B — suite 1; C/D — suite 3; E/F — suite 4 (Table 1). Post samples feature large, equant felsic minerals and tabular biotite, whereas host rock samples show ductile deformation fabrics, with feldspar porphyroblasts, recrystallized and ribbon quartz, and elongate biotite.

any discernible chemical changes. Whereas one might surmise that the ratio of base cations of high mobility (K_2O, N_2O, CaO, and MgO) to immobile cations (Al_2O_3,Fe_2O_3, and TiO_2) would be higher in samples from weathering posts than those from host rocks, no such trend is evident in the four sample suites measured (Fig. 7; Tables 1 and 3). It is possible that expected trends would be present if samples were focused on the upper several millimeters of the rock surface. The 4–5 cm-long cores that were obtained from the weathering posts and host rocks may simply have been too long; that is, they may have extended well into the fresh rock, thus effectively diluting the compositional influence of the true weathering front. However, this seems unlikely given the many meters of mobile element depletion in granodiorite that have been measured on some late Quaternary granodiorite surfaces (White et al., 2001).

One explanation for the lack of expected trends is that there simply is no accumulation of a weathering residue on the rock surfaces themselves. Chemical weathering may loosen the bonds between mineral grains, through the expansion of biotite and its eventual alteration to clay (cf. Isherwood and Street, 1976). The loosened grains may fall off or be blown off the boulder surface and continue their chemical alteration in the surrounding soil. This explanation has been proposed to explain the presence of weathering pits on fresh-appearing boulders above timberline in the Colorado Front Range (Birkeland, 1999). Pre-Holocene moraines in the Cordillera Blanca are mantled by between 8 and 45 cm (mean = 29 cm; n = 26) of what has been designated as a mixture of löess and till (Rodbell, 1993). This interpretation stemmed from the observation that surface horizons in soil profiles contain fewer cobbles, lower sand content, and higher clay content than horizons at depth (Rodbell, 1991). It is likely that some of the purported löess component is simply the partially altered remains of weathered granodiorite boulders. This would explain both the lack of any observable weathering rinds and the lack of any geochemical evidence of a weathering residue on granodiorite boulders.

https://doi.org/10.1016/j.yqres.2011.09.004 Published online by Cambridge University Press

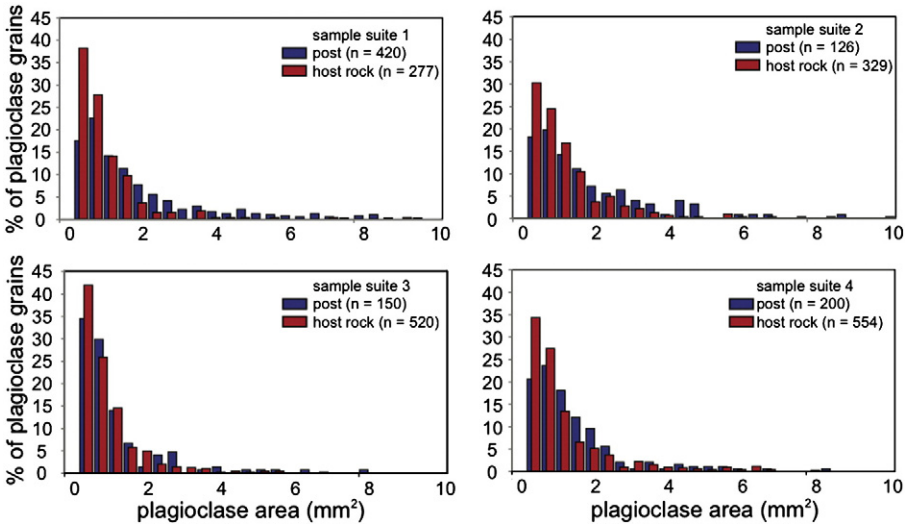

Figure 5. Plagioclase area for post and host rock samples from sample suites 1–4 (Table 1) for 2576 individual phenocrysts (Table 3). Plagioclase grains from host-rock samples are smaller than those from post samples.

Rate of development of weathering posts

The rate of weathering-post development is equal to the difference between the denudation rate of the surrounding host rock (D_R) and the denudation rate of the post (D_P), where $D_R > D_P$. As noted above, weathering posts have not been observed on Holocene moraines, and this may reflect the difficulty of discerning small weathering posts from cm-scale asperities on relatively fresh rock surfaces. However, over at least the past ~30 ka weathering posts have developed at an average rate of ~1.45 cm $(1000\ yr)^{-1}$ (Table 4; Fig. 8).

We estimate the uncertainty of this linear rate of post development by simply choosing combinations of post heights and moraine ages plus and minus the uncertainty of the moraine ages (Table 4). For the purposes of this estimate, we assume that the moraine ages in Table 4 have a ±20% uncertainty. Subtracting the uncertainty of the moraine age yields a higher rate of post development, and vice versa. Accordingly, the aforementioned average rate of post development over the past ~30 ka of ~1.45 cm $(1000\ yr)^{-1}$ should be considered to have an uncertainty of about ±30%, thus yielding a range between approximately 1 and 2 cm $(1000\ yr)^{-1}$.

The rate of post development beyond 30 ka is less clear, and this uncertainty stems from uncertainty over the age of the Cojup moraines that possess weathering posts ~66 cm tall. Sixteen CRN ages for the Cojup moraines generate probability density clusters at 75, 125, 225, and 440 ka (Farber et al., 2005). These authors suggest that these groupings may in fact record repeated glacial advances to a similar ice limit, thus generating a compound lateral moraine on the piedmont above the village of Huaraz (Fig. 1C). The highly denuded nature of this moraine and lack of any clear crest is consistent with this compound origin. If the oldest CRN age (440 ka) is used in the calibration curve (Fig. 7), then rates of post development appear to slow considerably beyond ~30 ka; average rates would be ~0.07 cm $(1000\ yr)^{-1}$ for the period 30–400 ka. Accordingly, the rate of post development would be best modeled by the logarithmic equation:

$$Y = 13.852^{*}\ln X - 12.420;\ r^2 = 0.88,$$

where Y is weathering post height (cm) and X is time (ka).

The observation that apparent rates of weathering-post development slow with time is consistent with numerous studies of the

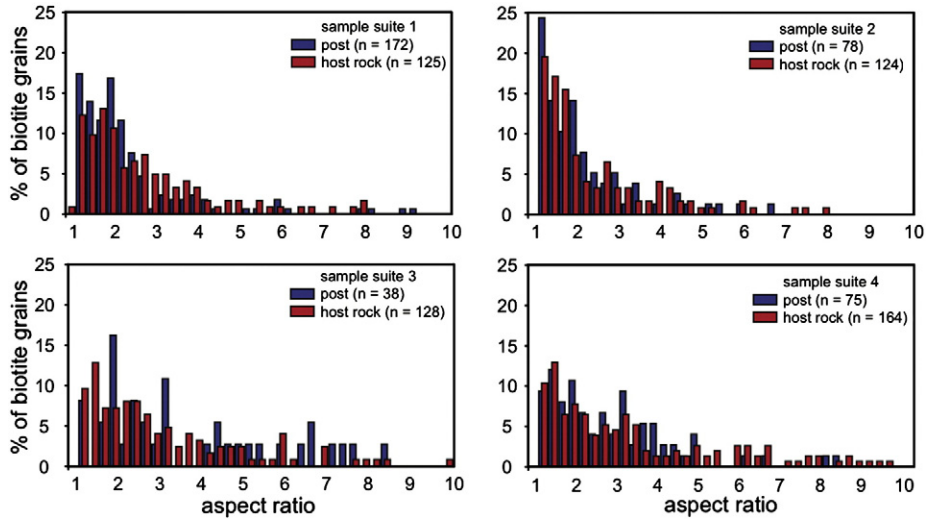

Figure 6. Biotite axial ratio for post and host rock samples from sample suites 1–4 (Table 1) for 904 individual phenocrysts (Table 3). Biotite grains from host rock samples show enhanced elongation relative to those from post samples.

https://doi.org/10.1016/j.yqres.2011.09.004 Published online by Cambridge University Press

Table 3
Area of plagioclase phenocrysts and aspect ratio of biotite phenocrysts in post and host rock samples.

Sample suite (Table 1)	Sample	Distance from post (cm)	Plagioclase area (mm^2)	Std dev	N (plagioclase)	Biotite aspect ratio	Std dev	N (biotite)
1	R93PE1	0	2.08	2.39	147	1.89	0.76	70
	R93PE2	0	1.96	2.6	122	2.42	1.52	46
	R93PE3	0	1.49	1.96	151	2.47	1.83	56
	R93PE4	10	1.09	1.25	109	2.88	2.1	38
	R93PE8	125	0.86	0.76	168	2.93	2.74	87
2	R93PE12	0	1.66	1.55	126	2.12	1.2	78
	R93PE10	20	1.31	2.58	166	2.51	1.72	76
	R93PE11	20	1.16	1.59	163	2.24	1.65	48
3	R93PE14	0	0.96	1.19	150	3.87	2.39	38
	R93PE15	25	0.8	0.79	266	3.31	2.6	73
	R93PE16	60	0.77	0.93	254	3.07	1.89	55
4	R93PE17	0	1.29	1.28	200	2.77	1.54	75
	R93PE18	5	1.08	1.28	229	2.72	1.83	56
	R93PE19	25	1.04	1.57	100	3.94	3.16	57
	R93PE20	50	1.07	1.36	225	4.65	3.49	51

functional relationship between weathering rates and time (e.g., Colman, 1981; Birkeland, 1999). Colman (1981) asserted that declining rates of weathering with time reflect the fact that silicate minerals dissolve incongruently, thus leaving some type of residue behind, which reduces the exposure of unaltered minerals to water and organic acids, and impedes further chemical removal from fresh mineral grains. Weathering rates should become linear only when an equilibrium thickness of residue has been reached, and this may take on the order of 500 ka for some weathering phenomena (Colman, 1981), which may be true in this case.

However, as noted above, no weathering rinds or geochemical evidence of weathering residues have been observed on any of the samples collected in this study. Thus, incongruent weathering of silicates may not be operative, and the apparent decline in weathering-post development with time (Fig. 8) is simply due to an incorrect age assignment for the Cojup moraines. If the youngest clustering of CRN ages (~75 ka) for the Cojup moraines is used in Figure 8, then a linear rate of 0.9 cm $(1000\ yr)^{-1}$ for the past ca. 75 ka is plausible. This rate is similar to the lower limit of the aforementioned average rate of post development over the past 30 ka of 1.45 ± 0.45 cm $1000\ (yr)^{-1}$. A more or less constant rate of post development between 1 and 2 cm $(1000\ yr)^{-1}$ is consistent with the observed absence of a weathering residuum on boulder surfaces.

One factor that clearly influences apparent rates of weathering-post development is simply the size of the posts themselves. Post development must stop completely when the size of a weathering post reaches the diameter of the original host rock. Given the aforementioned initial linear rate of weathering-post development of $\sim 1.45 \pm 0.45$ cm $(1000\ yr)^{-1}$ and typical boulder diameters of ~1.5 m, the upper limit on the growth period of weathering posts is ~100 ka. It follows that older moraines would not have boulders with significantly larger weathering posts unless they also possessed significantly larger boulders. At least one example of this has been located on an undated left-lateral moraine >400 ka (Farber et al., 2005) on the piedmont above the village of Huaraz. Here one very large boulder (long axis>8 m) possesses a weathering post that is about 1.5 m tall (Fig. 2*f*). Thus, according to this scenario, the rate of post development is, in fact, linear; the apparent reduction in the rate of post development is due to the scarcity of boulders with diameters that exceed 1.5 m on moraines >100 ka.

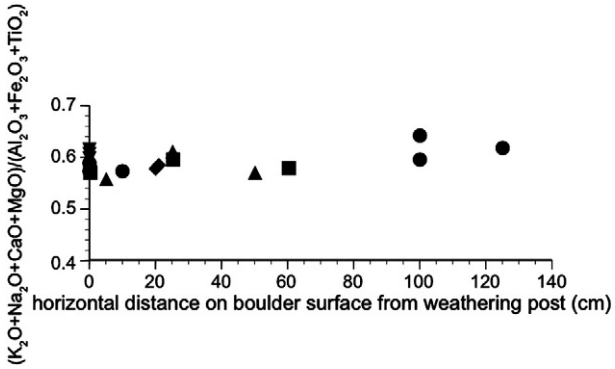

Figure 7. Variation in ratio of mobile to immobile cations with increasing horizontal distance from weathering posts in four suites of samples. Suite 1 is denoted by circles, suite 2 by diamonds, suite 3 by squares, and suite 4 by triangles.

Implications for CRN exposure dating in the Cordillera Blanca

Inasmuch as D_R must exceed D_P, and $D_R - D_P = 1.45 \pm 0.45$ cm $(1000\ yr)^{-1}$ for much of the late Quaternary, the erosion of granodiorite boulders (DR) could impart a significant error on CRN exposure ages in the Cordillera Blanca if such erosion rates are not taken into account. These errors, as a percentage of the exposure age, increase significantly with the age of the substrate. For example, an unrecognized erosion rate of 1.45 cm $(1000\ yr)^{-1}$ using the CRONUS-Earth Online Calculator v. 2.2 (Balco et al., 2008) and data from Smith and Rodbell (2010) for a boulder on a late-glacial moraine (~13 ka) would result in a CRN exposure age that underestimates the true age by 19%. Similarly, an unrecognized erosion rate of 1.45 cm $(1000\ yr)^{-1}$ on a moraine from the local last glacial maximum (~30 ka) would result in CRN exposure ages that underestimate the true age by ~43%. Given that the erosion rate of 1.45 cm $(1000\ yr)^{-1}$ is a minimum-limiting erosion rate for post generating host rocks, the resultant age error is also a minimum estimate. Whereas workers sampling for CRN exposure ages would almost certainly avoid rocks with large weathering posts, the erosion rate of granodiorite boulders that lack weathering posts, as some do, could be underestimated because such boulders commonly lack other evidence (e.g., grussification, weathering pits and rinds) of deep weathering.

To evaluate the potential impact of substantial unrecognized erosion of granodiorite boulders on resultant CRN exposure ages from the Cordillera Blanca, we evaluate the data set of 60 ^{10}Be exposure ages from Smith and Rodbell (2010). In this study, 20% of the exposure ages are from quartzite boulders that possess glacial striae and glacial polish, 65% are from granodiorite boulders, and 15% are from felsic volcanic rocks. All of the boulders of the latter two rock types that were sampled lack weathering posts but are also devoid of glacial polish and striae. One would expect that given the fresh appearance of the quartzite boulders these boulders would yield consistently older CRN ages. However, data from the six moraines that contain mixed lithologies reveal no systematic CRN age differences among the three rock types. Among samples from the same moraine, exposure ages from ganodiorite boulders are as likely to be older than

https://doi.org/10.1016/j.yqres.2011.09.004 Published online by Cambridge University Press

Table 4
Calibration data used in estimating rates of weathering post development.

Moraine	Number of moraines	Estimated moraine age (ka)	20% uncertainty of moraine age estimate (ka)	Weathering post height-mean of 5 largest (cm)	Standard deviation of mean weathering post height (cm)
Moraines on the west side of the Nevado Jeulla Rajo Massif (Smith and Rodbell, 2010)					
M2 right lateral	1	32	4.8	45.3	13.7
M2 left lateral	1	32	4.8	36.0	6.0
M3 right lateral	1	18	2.7	26.5	2.7
M3 left lateral	1	18	2.7	25.2	3.7
M4 left lateral	1	16.5	2.5	28.2	7.2
M5 left lateral	1	15	2.3	24.4	3.7
Moraines on the Huaraz-Catac Piedmont (Rodbell, 1992; Farber et al., 2005)					
Gueshque II	2	0.1	0.012	0.0	0.0
Gueshque I	4	0.7	0.105	0.0	0.0
Quilloc	6	2.2	0.33	0.0	0.0
Rio Negro	3	7.5	1.1	0.0	0.0
Manachaque	7	10.0	1.5	12.0	2.0
Laguna Baja	7	16.5	2.5	23.0	2.0
Rurec	6	29.0	4.4	42.0	5.0
Cojup	2	>400	60.0	66.0	5.0

their quartzite counterparts as they are to be younger. Apparently, the granodiorite boulders sampled were not subject to the high boulder erosion rate (DR) noted above. That these same boulders also lack weathering posts suggests that there may be more than one population of granodiorite boulders on moraine crests in the Cordillera Blanca. Those boulders that possess weathering posts do so because they possess the mylonite texture noted above that is conducive to accelerated chemical and physical weathering throughout most, but not all, of the boulder. However, apparently at least some of the boulders that do not possess weathering posts have mineral textures that are similar to those of weathering posts themselves and thus weather at a rate that is much lower than the differential weathering rate (DR) of 1.45 ± 0.45 cm $(1000\ \mathrm{yr})^{-1}$. In summary, then, it is the sporadic presence of mylonite textures in granodiorite boulders that generates the localized high rates of differential boulder denudation responsible for weathering-post development; CRN samples from boulders that lack such textures and those from the tops of weathering posts should yield similar ages to one another, and these should closely approximate the age of moraine stabilization.

Conclusions

Weathering-post development on granite and granodiorite erratics in the Cordillera Blanca Peru occurs due to differential weathering that is the result of subtle differences in texture. Thin sections reveal that host rocks have veins of micro-crystalline quartz surrounded by ribbons of biotite that flow around feldspar phenocrysts; these are absent in thin sections from weathering posts. Smaller grain sizes and a greater biotite axial ratio in host rocks are apparently responsible for the higher rate of surface denudation in host rocks relative to weathering posts. These textural differences are likely the result of mylonitization related to multiple generations

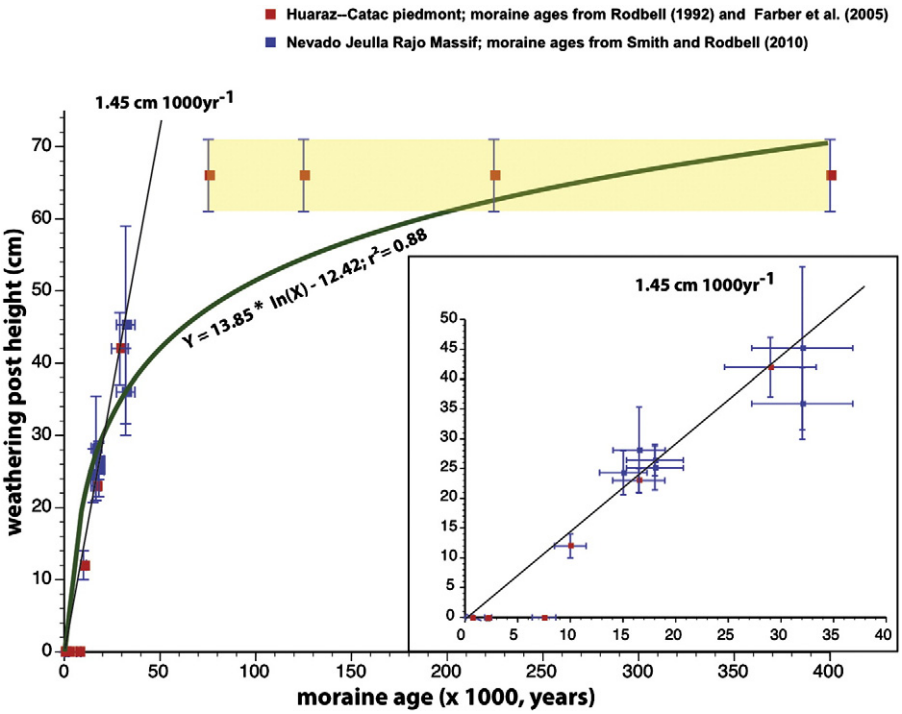

Figure 8. The development of weathering posts with time on late Quaternary moraines on the west side of the Cordillera Blanca, Peru. Y-axis is the mean of the five largest weathering posts on moraine crests. Inset highlights weathering-post development over the past 40 ka. Yellow box illustrates range of four possible ages for moraine with 66 cm-tall weathering posts.

https://doi.org/10.1016/j.yqres.2011.09.004 Published online by Cambridge University Press

of batholith emplacement on the west side of the Cordillera Blanca. Expansion of biotite in host rocks due to chemical weathering thus creates long, continuous cracks that serve as avenues for the infiltration of weathering solutions.

The absence of consistent trends in major- or trace-element geochemistry between post and host rock samples indicates that there is no accumulation of a weathering residue on rock surfaces. Apparently, the loosening of grain boundaries in response to the expansion of biotite results in grains falling off boulder surfaces and continuing their chemical alteration in the surrounding soil.

Moraines dated by radiocarbon and/or ^{10}Be provide the basis for calibrating the rate of weathering-post development. Accordingly, weathering posts appear to develop at the linear rate of $1.45\,\mathrm{cm} \pm 0.45$ 1000^{-1} yr until post height reaches the diameter of the host rock. Thus, weathering posts can provide a useful numeric dating tool for the west side of the Cordillera Blanca for landforms containing granite and granodiorite boulders deposited in the last 100,000 yr.

Our work suggests that the absence of a weathering post on a granite or granodiorite boulder in the Cordillera Blanca indicates that the boulder does not have the mylonitic textural properties that would make it susceptible to weathering-post development. One implication for paleoclimate reconstruction in the Cordillera Blanca is that moraine ages obtained through CRN dating of boulders that lack weathering posts (or through CRN dating of weathering posts themselves) are likely to be similar to CRN ages from quartzite boulders that still possess glacial polish and striae. Both sets of ages can provide accurate estimates of the age of moraine stabilization.

Acknowledgments

We are grateful to students in the 2009 Union College miniterm course *Impacts of Climate Change to the Cordillera Blanca* for help in measuring weathering posts. We thank the Ames family and Frederico Manrique of Huaraz, Peru, for many years of hospitality and logistical assistance, and William Neubeck of the Union College Geology Department for preparing thin sections.

References

Atherton, M.P., Sanderson, L.M., 1987. The Cordillera Blanca Batholith: a study of granite intrusion and the relation of crustal thickening to peraluminosity. Geologische Rundschau 76, 213–232.

Balco, G., Stone, J.O.H., Lifton, N.A., Dunai, T.J., 2008. A complete and easily accessible means of calculating surface exposure ages or erosion rates from ^{10}Be and ^{26}Al measurements. Quaternary Geochronology 3, 174–195.

Birkeland, P.W., 1973. Use of relative age-dating methods in a stratigraphic study of rock glacier deposits, Mt. Sopris, Colorado. Arctic and Alpine Research 5, 401–416.

Birkeland, P.W., 1974. Pedology, Weathering, and Geomorphological Research. Oxford University Press, New York.

Birkeland, P.W., 1999. Soils and Geomorphology. Oxford University Press, New York.

Birkeland, P.W., Colman, S.W., Burke, R.M., Shroba, R.R., Meierding, T.C., 1979. Nomenclature of alpine glacial deposits, or what's in a name? Geology 7, 532–536.

Blackwelder, E., 1931. Pleistocene glaciation in the Sierra Nevada and Basin Ranges. Geological Society of America Bulletin 42, 865–922.

Bland, W., Rolls, D., 1998. Weathering: Introduction to the Scientific Principles. Oxford University Press, New York.

Burbank, D.W., Cheng, K.J., 1991. Relative dating of Quaternary moraines, Rongbuk Valley, Mount Everest, Tibet: implications for an ice sheet on the Tibetan Plateau. Quaternary Research 36, 1–18.

Burke, R.M., Birkeland, P.W., 1979. Reevaluation of multiparameter relative dating techniques and their application to the glacial sequence along the eastern escarpment of the Sierra Nevada, California. Quaternary Research 11, 21–51.

Chinn, T.J.H., 1981. Use of rock weathering-rind thickness for Holocene absolute age-dating in New Zealand. Arctic and Alpine Research 13, 33–45.

Clapperton, C.M., 1981. Quaternary glaciations in the Cordillera Blanca, Peru and the Cordillera Real, Bolivia. Memoria del Primer Seminario Sobre el Cuaternario de Colómbia. Revista Centro Interamericano de Fotointerpretacíon C.I.A.F, Bogotá, pp. 93–111.

Colman, S.M., 1981. Rock-weathering rates as functions of time. Quaternary Research 15, 250–264.

Colman, S.M., Pierce, K.L., 1980. Weathering rinds on andesitic and basaltic stones as a Quaternary age indicator, western United States. U.S. Geological Survey Professional Paper 1210.

Eggler, D.H., Larson, E.E., Bradley, W.C., 1969. Granites, grusses, and the Sherman erosion surface, southern Laramie Range, Colorado-Wyoming. American Journal of Science 267, 510–522.

Farber, D.L., Hancock, G.S., Finkel, R.C., Rodbell, D.T., 2005. The age and extent of tropical alpine glaciation in the Cordillera Blanca, Peru. Journal of Quaternary Science 759–776.

Gapais, D., 1989. Shear structures within deformed granites: mechanical and thermal indicators. Geology 17, 1144–1147.

Gosse, J.C., Phillips, F.M., 2001. Terrestrial in situ cosmogenic nuclides: theory and application. Quaternary Science Reviews 20, 1475–1560.

Isherwood, D., Street, A., 1976. Biotite-induced grussification of the Boulder Creek granodiorite, Boulder County, Colorado. Geological Society of America Bulletin 87, 366–370.

Petford, N., Atherton, M., 1992. Granitoid emplacement and deformation along a major crustal lineament: the Cordillera Blanca, Peru. Tectonophysics 205, 171–185.

Pierce, K.L., Obradovich, J.D., Friedman, I., 1976. Obsidian hydration dating and correlation of Bull Lake and Pinedale glaciations near West Yellowstone, Montana. Geological Society of America Bulletin 87, 703–710.

Rodbell, D. T., 1991. Late Quaternary glaciation and climatic change in the northern Peruvian Andes. Unpublished PhD. thesis, University of Colorado.

Rodbell, D.T., 1992. Lichenometric and radiocarbon dating of Holocene glaciation, Cordillera Blanca Perú. The Holocene 2, 19–29.

Rodbell, D.T., 1993. Subdivision of late Pleistocene moraines in the Cordillera Blanca, Peru, based on rock-weathering features, soils, and radiocarbon dates. Quaternary Research 39, 133–143.

Schwartz, D.P., 1988. Paleoseismicity and neotectonics of the Cordillera Blanca Fault Zone, northern Peruvian Andes. Journal of Geophysical Research 93, 4712–4730.

Segall, P., Simpson, C., 1986. Nucleation on ductile shear zones on dilatant fractures. Geology 14, 56–59.

Servicio Nacional de Geología y Minería, 1970. Mapa geológico del Departamento de Ancash (1:250,000). Ministerio de Energía y Minas, Lima.

Smith, D. N., 1988. Flora and vegetation of the Huascarán National Park, Ancash, Peru with preliminary taxonomic studies for a manual of the flora. Unpublished Ph.D. thesis, Iowa State University.

Smith, J.A., Rodbell, D.T., 2010. Cross-cutting moraines reveal evidence for North Atlantic influence on glaciers in the tropical Andes. Journal of Quaternary Science 25, 243–248.

Vernon, R.H., Williams, V.A., D'arcy, W.F., 1983. Grain-size reduction and foliation development in a deformed granitoid batholith. Tectonophysics 93, 123–145.

White, A.F., 2002. Determining mineral weathering rates based on solid and solute weathering gradients and velocities: application to biotite weathering in saprolites. Chemical Geology 190, 69–89.

White, A.F., Bullen, T.D., Schulz, M.S., Blum, A.E., Huntington, T.G., Peters, N.E., 2001. Differential rates of feldspar weathering in granitic regoliths. Geochimica et Cosmochimica Acta 65, 847–869.

Whitehouse, I.E., McSaveney, M.J., Knuepfer, P.L.K., Chinn, T.J., 1986. Growth of weathering rinds on torlesse sandstone, Southern Alps, New Zealand. In: Colman, S.M., Dethier, D.P. (Eds.), Rates of Chemical Weathering of Rocks and Minerals. Academic Press, San Diego, pp. 419–435.

Wilson, J., Reyes, L., Garayar, J., 1967. Geología de los cuadrangulos de Mollebamba, Tayabamba, Huaylas, Pomabamba, Carhuaz, y Huari. Servicio de Geología y Minería Boletín, 16.